REPORT DOCUMENTATION PAGE	Form Approved OMB No. 0704-0188

PLEASE DO NOT RETURN YOUR FORM TO THE ABOVE ORGANIZATION.

1. REPORT DATE (DD-MM-YYYY)	2. REPORT TYPE	3. DATES COVERED (From - To)
05-08-2009	Conference Proceeding	

4. TITLE AND SUBTITLE	5a. CONTRACT NUMBER
Are Sulfate Reducing Bacteria Important to the Corrosion of Stainless Steels?	5b. GRANT NUMBER
	5c. PROGRAM ELEMENT NUMBER 0601153N
6. AUTHOR(S) Jason S. Lee, Richard I. Ray, Brenda J. Little	5d. PROJECT NUMBER
	5e. TASK NUMBER
	5f. WORK UNIT NUMBER 73-5052-18-5

7. PERFORMING ORGANIZATION NAME(S) AND ADDRESS(ES)	8. PERFORMING ORGANIZATION REPORT NUMBER
Naval Research Laboratory Oceanography Division Stennis Space Center, MS 39529-5004	NRL/PP/7330-08-8246
9. SPONSORING/MONITORING AGENCY NAME(S) AND ADDRESS(ES)	10. SPONSOR/MONITOR'S ACRONYM(S)
Office of Naval Research 800 N. Quincy St. Arlington, VA 22217-5660	ONR
	11. SPONSOR/MONITOR'S REPORT NUMBER(S)

12. DISTRIBUTION/AVAILABILITY STATEMENT

Approved for public release, distribution is unlimited

13. SUPPLEMENTARY NOTES

14. ABSTRACT

Testing susceptibility of stainless steels to abiotic sulfide derivatization in a chloride-containing medium under laboratory conditions was directly related to the types and concentrations of alloying elements. Derivatization decreased in the following order 430>304L>316L>904L. Laboratory results compared favorably with electrochemical model predictions. Results of the testing and modeling will be used to refine models for the impact of microbiologically produced sulfides on stainless steels.

15. SUBJECT TERMS

stainless steels, sulfide derivatization, marine corrosion, modeling

16. SECURITY CLASSIFICATION OF:			17. LIMITATION OF ABSTRACT	18. NUMBER OF PAGES	19a. NAME OF RESPONSIBLE PERSON
a. REPORT	b. ABSTRACT	c. THIS PAGE			Jason Lee
Unclassified	Unclassified	Unclassified	UL	13	19b. TELEPHONE NUMBER (Include area code) 228-688-4494

Paper No.
3107

ARE SULFATE REDUCING BACTERIA IMPORTANT TO THE CORROSION OF STAINLESS STEELS?

J. S. Lee and R.I. Ray
Naval Research Laboratory, Stennis Space Center, MS 39529, Code 7332

B. J. Little
Naval Research Laboratory, Stennis Space Center, MS 39529, Code 7303

ABSTRACT

Testing susceptibility of stainless steels to abiotic sulfide derivitization (10^{-2} M) in a chloride-containing medium under laboratory conditions was directly related to the types and concentrations of alloying elements. Derivatization decreased in the following order 430 > 304L > 316L > 904L. Laboratory results compared favorably with electrochemical model predictions. Results of the testing and modeling will be used to refine models for the impact of microbiologically produced sulfides on stainless steels.

Keywords: stainless steels, sulfide derivatization, marine corrosion, modeling

INTRODUCTION

Sulfate reduction that leads to sulfide derivatization of susceptible metals has been studied intensely since the 1980's. Despite the extensive literature on sulfate reduction in seawater it is impossible to make predictions as to the impact sulfides exert on low alloy (e.g., 304 and 316) and medium grade (e.g., 317, 904) stainless steels exposed in marine environments. Previous laboratory experiments designed to provide data on susceptibility of steels to sulfide derivatization have produced conflicting results. Experiments reported in this paper were designed to determine the susceptibility of a variety of stainless steels to sulfide derivatization and to further determine the role of alloying elements in decreasing this susceptibility. Results of the laboratory experiments were compared with results obtained when applying a thermodynamic/electrochemical model.

MATERIALS AND METHODS

Sulfide was employed to convert surface metal oxide to metal sulfide on steel specimens. Concentration of sulfide used was 10^{-2}M for direct comparison to the McNeil/Odom model[1] which predicts sulfide mineral formation. Upon acid cleaning of test specimens, metal sulfides formed from derivatization were removed and a weight loss of specimens recorded. Control samples were used to separate the inherent weight loss from the loss due to the cleaning procedure.

Exposure Media

Artificial seawater (ASW) was produced by mixing a commercially available mixed salt and distilled water (dH_2O) to a measured salinity of 35 parts-per-thousand (ppt). The ASW was vacuum drawn through a No. 42 filter and pH was adjusted to 8.0 value using 1.2 N hydrochloric acid. ASW, in volumes of 2 liters, was bubbled with nitrogen gas (N_2) for 30 minutes to remove dissolved oxygen (O_2). During nitrogen purging the pH value increased to > 9.5 due to the removal of carbon dioxide (CO_2).

Deaerated ASW was then placed in an anaerobic hood with an atmospheric composition of 10% hydrogen, 0.1% CO_2 with the balance N_2. A constant temperature of 25°C was maintained. The ASW was stirred and the anaerobic atmosphere was bubbled into the ASW for 30 minutes. The pH value returned to that between 7.9 and 8.0. Two 2000 mL crystallization dishes were filled with 2L of ASW each. Another crystallization dish was filled with 2L of dH_2O that underwent the same bubbling treatments as the ASW samples. All three dishes were placed on a shaker table which rotated at 60 revolutions-per-minute. To one of the 2L ASW samples, 4.8037 g of sodium sulfide nonahydrate ($Na_2S{\cdot}9H_20$) was added to give a final sulfide (S^{-2}) concentration of 10^{-2} M.

Metal Coupons

Four stainless steels were chosen for these experiments:

- UNS S43000 (430) - Fe-17Cr alloy
- UNS S30403 (304L) - Fe-19Cr-10Ni
- UNS S31603 (316L) - Fe-17Cr-13Ni-3Mo
- UNS N08904 (904L) - Fe-21Cr-26Ni-6Mo

These alloys were selected for their differences in bulk alloy chemistry, specifically, increasing amounts of alloying elements, i.e. chromium (Cr), nickel (Ni) and molybdenum (Mo).

Stainless steel coupons (1.59 cm diameter and 0.16 cm thickness) were wet polished to 600 grit finish, rinsed sequentially in acetone then methanol and air-dried. Weight in grams (g) was recorded for each sample to the fourth decimal place using an analytical balance.

Exposure and Cleaning

For each of the 4 alloys, three pre-weighed coupons were placed into each of the 3 different exposure media (dH_2O, ASW, ASW+S^{-2}) giving a total of 36 coupons. No external polarization was applied; all experiments were conducted at an open circuit potential. After 65 hours, each coupon was removed from its respective exposure medium and placed into a separate falcon tube. Corrosion products, iron oxides and sulfides, were removed following ASTM Standard G1 procedures[2]. The C.7.5 designation of the G1 procedure was used. Each sample was bathed for 5 min in a solution of 100 mL of concentrated nitric acid (1.42 specific gravity), 20 mL hydrofluoric acid (48%-1.198 specific gravity) and reagent water to make 1000 mL. Following the acid wash, each coupon was rinsed in three

consecutive dH_2O baths with a final rinse in pure methanol. The coupons were dried with N_2, weighed, and examined under an optical microscope at magnification of up to 50X.

Modeling

A commercially available program,[†] consisting of a thermodynamic model and an electrochemical module, was used to calculate corrosion rates[3] and potential-pH stability diagrams[4] (Pourbaix diagrams) for each of the three exposure conditions. Settings for each modeled solution were adjusted to pH value of 8.0 and temperature of 25°C to match the experimental conditions. ASW was modeled using major ion concentrations taken from the literature[5] for natural seawater with a salinity of 35 ppt., as listed in Table 1. For the ASW+S^{-2} exposure, 0.01M $Na_2S{\cdot}9H_2O$ (2396 ppm) was added to the calculation. Distilled water was modeled as being ion free.

The software library included electrochemical behavior of types 304 and 316 stainless steels for direct corrosion rate determination of experimental alloys 304L and 316L. However, the software library did not contained electrochemical data for alloys 430 and 904L. A Fe-13Cr stainless steel was available and was chosen to represent alloy 430 (Fe-17Cr). This choice is considered a good compromise since stainless steels are defined as having greater than 12% Cr.. Below 12% Cr, an Fe-Cr alloy has predominantly iron oxide on its surface, while with about 12% Cr, the oxide becomes mainly chromium oxide. UNS S31254 (Fe-20Cr-18Ni-6Mo) was chosen to represent alloy 904L (Fe-21Cr-26Ni-6Mo) having the closest chemical composition to that available in the software library.

Stability diagrams were generated for the dH2O exposure conditions with 10^{-2}M sulfide addition for each alloy. The ASW+S2- exposure condition was not used in stability diagram generation due to the complex chemical nature of seawater which would result in large numbers of possible solids,thus rendering the diagrams difficult to read. Unlike corrosion rate determination, all of the experimental alloys were available for modeling since only the bulk chemical composition of each alloy was needed for these calculations. Each transition metal (Fe, Cr, Ni, Mo), as well as sulfur, were capable of undergoing redox reactions, *i.e.,* had variable valence states. The software allowed suppression of individual solids formation during calculation of stability diagrams[6].

RESULTS AND DISCUSSION

Weight Loss and Corrosion Rates

Figure 1 shows average weight loss data for each alloy exposed under the three different deaerated conditions: ASW+ S^{-2}, ASW, and dH_2O. In general, exposure to ASW+ S^{-2} resulted in the highest weight loss for each alloy, with the exception of 904L, for which the highest weight loss was recorded in ASW. It should be noted that each of the three 430 samples had the same recorded weight loss to the fourth decimal place. Increase in ionic content and electrolyte conductivity from dH_2O to ASW did not produce any significant trend in weight loss across the different alloys. These results suggest that anions such as Cl^- or SO_4^{2-} in ASW did not increase weight loss from acid cleaning. Increasing alloying content resulted in decreased weight loss where 430 steel had the highest weight loss with the lowest amount of alloying. The opposite was observed for 904L steel.

Corrosion rates calculated from modeling work are shown in Figure 2. In general, the same trends are observed as for experimentally obtained weight loss results, presented in Figure 1. One exception is the two orders-of-magnitude higher corrosion rate for 430 exposed to ASW+S^{-2} in

[†] Corrosion Analyzer v.2.0.58, OLI System, Inc., Whipanny, NJ

comparison to other alloy/exposure conditions. Another exception is that 430 had lower corrosion rates in ASW and dH_2O when compared to 304L. One explanation could be that while the model employed an Fe-13Cr stainless steel in calculating corrosion rates for 430, the experimental alloy was Fe-17Cr. The decrease in Cr content may have resulted in an oxide that underwent sulfur derivatization more easily than the alloy with the higher Cr concentration. In agreement with the experimental results presented in Figure 1, the model predicted that the highest alloyed stainless steel S31254 (substituted for 904L) would have its highest corrosion rate in ASW and not ASW+S^{-2}. No explanation for this result is offered at this time.

Optical microscopy examination of steel specimens, up to magnification of 50X, revealed that none of 430 and 304L coupons retained any polishing marks. The surfaces showed an even dispersal of <25 micron diameter pits. Samples exposed to ASW+S^{-2} had the densest pit population. Coupons manufactured from alloy 316L retained the majority of surface polishing marks with only a few distinguishable pits that were dispersed unevenly, regardless of the type of exposure media. At the reported magnification, alloy 904L showed no signs of pitting.

Figures 3-6 show stability diagrams for 10^{-2}M sulfide and alloys 430, 304L, 316L, and 904L, respectively. The Fe subsystem is the major component in each diagram, where only iron containing minerals are shown. The Cr subsystem is also shown to illustrate the region of protection the chromium oxide (Cr_2O_3) provides. The Ni subsystem for 304L, 316L, and 904L is not shown nor is the Mo subsystem for 316L and 904L for simplicity. Each figure indicates that the stable formation of iron sulfides is possible at the experimental pH range of 7.9-8.0. The iron sulfides are pyrite (isometric FeS_2) and pyrrhotite (hexagonal FeS). During stability diagram calculation, formation of iron sulfides marcasite (orthorhombic FeS_2), mackinawite (tetragonal FeS) and amorphous FeS were suppressed. Marcasite formation has not been shown to occur in the natural environment, while mackinawite has been demonstrated to be formed only in the presence of microbial activity such as sulfate-reducing bacteria[7]. While neither the Ni or Mo subsystem in shown in Figures 3-6, redox reactions involving Ni and Mo subsystems did account for changes in the pyrrhotite stability region. The maximum pH values at which pyrrhotite is stable are 8.55 for alloy 430, 8.44 for alloy 304L, 8.53 for alloy 316L, and 8.34 for alloy 904L. Stability diagrams (Figures 3-6) indicate that the assessment of susceptibility to sulfide derivatization for each alloy requires additional data, including sulfide formation kinetics and differences between bulk and surface chemistries.

Susceptibility of silver, carbon steel, copper, nickel and lead to derivatization by microbiologically produced sulfides is predicted by a thermodynamic model proposed by McNeil and Odom.[1] The model for predicting SRB influenced corrosion (SRB-MIC) is based on the likelihood that a metal would react with microbiologically produced sulfide. The model assumes that SRB-MIC is initiated by sulfide-rich reducing conditions in the biofilm and that under those conditions the oxide layer on the metal (or the metal itself) is destabilized and acts as a source of metal ions. At the outer surface of the SRB cell wall sulfide ions react to produce sulfide compounds in micron-sized particles that, in some cases, are crystalline. The oxidation/reduction of metal ions at bacterial surface is balanced by the release of surface ions until the oxide is totally consumed. If the reaction to convert the metal oxide to a metal sulfide has a positive Gibbs free energy under surface conditions, the sulfides will not strip the protective oxide and corrosion will not take place. If, however, the Gibbs free energy for this reaction is negative, the reaction will proceed. Sulfide microcrystals will redissolve and reprecipitate as larger, generally more sulfur-rich crystals, ultimately altering the chemistry of sulfide minerals stable under biofilm conditions.

McNeil/Odom[1] model predicts that the rate of sulfide mineral formation from stainless steels will be slower than for pure iron and that stainless steels with more than 6% molybdenum will be very resistant to derivatization. The model does not make specific predictions for low and medium grade stainless steel alloys. Laboratory experiments have attempted to provide such data, however, the literature on the subject of SRB influenced corrosion of passive alloys, particularly stainless steels with less than 6% Mo, is contradictory. For example, Brossia and Yang[8] exposed S30400 stainless steel in a deaerated (via N_2 bubbling) 0.5 M NaCl solution with an SRB (*Desulfovibrio vulgaris)* and a slime-forming bacterium (*Vibrio natrigens*). They added unspecified nutrients. They did not observe any significant corrosion. Yang and Cragnolino[9] exposed S30400 and S30403 to the same solution inoculated with the same organisms. No pitting was observed on either material. The authors specified that modified Baar's broth medium and NaCl nutrient broth were added to the test cells. The modified Baar's broth contained 1 gram L^{-1} yeast extract. The test cell was not deaerated. Webster *et al.*[10] concluded that SRB influenced corrosion in stainless steel is unlikely to occur in the absence of oxygen in the bulk electrolyte. The authors concluded that cathodic current provided by the oxygen reduction reaction (ORR) at discrete cathodic sites was required for high rates of anodic dissolution. In contrast, Neville and Hodgkiess[11] evaluated corrosion of five stainless steels (S32760, S31803, S31603, S31254 and a 25% Cr duplex) in a variation of Postgate's B medium (0.1% yeast extract), inoculated with SRB. The medium was deaerated with bubbling nitrogen. They reported increased susceptibility to localized and general corrosion in marine environments containing SRB for duplex and austenitic grades of stainless steels, even in the absence of an efficient ORR cathode.

The reason for the conflicting results may be due to varying laboratory conditions and varying media used to represent seawater. Two media are frequently used for SRB experiments 1) a variation of Postgate B medium and 2) artificial or natural seawater to which nutrients and microorganisms are added. The relative consistency of natural seawater[5] has led to the development of recipes for artificial seawaters. It is generally recognized that artificial seawater mixtures do not reproduce the complexity of natural seawater, especially the organic material. Dexter[12] concluded that synthetic seawater solutions were not free from organics. Instead, the organics were just different from those found in natural seawater. Webster and Newman[13] examined the impact of media constituents on localized corrosion of Fe-15Cr-10Ni stainless steel crevices and made the following observations: localized corrosion would not readily occur unless chloride (Cl^-) was the predominant anion in the medium. They concluded that Cl^- must be present in a concentration at least comparable to that of all other anions combined, otherwise corrosion was inhibited even at high H_2S concentrations up to 100 ppm. Reduction of the ratio of Cl^- to other anions increased the time to initiation and decreased the rate of propagation of the corrosion. Other corrosion investigators have concluded that extra nutrients cannot be added to stimulate bacterial growth if those nutrients inhibit corrosion by adding too many non-chloride ions.[14] Anions, including sulfate, hydroxide, phosphate, acetate, carbonate and nitrate can inhibit pitting corrosion. It is possible that bacterial consumption and fixation of nutrients, including sulfate could render an initially inhibiting solution aggressive by removing non-chloride ions.[15]

An additional complication in the interpretation of electrochemical measurements in synthetic media is the effect of culture media on the measurement. Webster and Newman[13] observed interferences in electrochemical measurements when yeast extract was included in the culture medium/electrolyte. The interferences were removed when the yeast extract was omitted.

A third standard practice that can influence the outcome of an experiment using marine SRB is the method of deaeration. Lee *et al.*[16] demonstrated dramatic changes in the chemistries and microflora of two natural coastal seawaters as a result of storage and environmental conditions. Exposure to an anaerobic atmosphere containing a mixed gas of 10% H_2, 5% CO_2, and balance N_2, generated the

highest number of SRB and dissolved sulfide concentrations. In contrast, sulfides and SRB were not detected in anaerobic seawater maintained with bubbled N_2. Lee *et al.*[16] demonstrated that bubbling N_2 into natural seawater produced a shift in pH values from 8.0 to above 9.0, creating an environment that was not conducive to the growth of SRB. Maintenance of seawater in an anaerobic hood with an anaerobic mixture of gases produced a pH shift from 8.0 to below 7.0 and a significant increase in SRB numbers as measured in a liquid culture using a dilution to extinction technique.

The McNeil/Odom model[1] is limited to thermodynamic predictions as to whether or not a reaction will take place and does not consider metal toxicity to the organisms, tenacity of the resulting sulfide or other factors that influence corrosion rates. The model predicts that copper alloys and carbon steel will be derivatized and predicts the conversion of the metal oxides to specific sulfide-containing minerals. Alloy 304 should not be used in seawater because of the propensity for crevice corrosion. However, the material does not appear to be vulnerable to sulfide derivatization.

CONCLUSIONS

- Electrochemical corrosion rate models accurately predict the susceptibility of stainless steels to abiotic sulfide derivatization in chloride-containing media.
- The thermodynamic stability models do not provide definitive susceptibilities to sulfide derivatization for specific stainless steel alloys.

ACKNOWLEDGEMENTS

This work was supported by the Office of Naval Research Program Element 0601153N (6.1 Research Program). NRL Publication Number NRL/JA/7303/##/####.

REFERENCES

1. M. B. McNeil, A. L. Odom, "Thermodynamic prediction of microbiologically influenced corrosion (MIC) by sulfate-reducing bacteria (SRB)," in Microbiologically Influenced Corrosion Testing, Vol. STP 1232, eds. J. R. Kearns and B. J. Little (Philadelphia, PA: ASTM, 1994), p. 173-179.

2. ASTM, "Standard G 1-90 - Standard practice for preparing, cleaning, and evaluating corrosion test specimens," in Annual Book of ASTM Standards, Vol. 3.02 (Phildelphia, PA: ASTM, 1993), p. 33.

3. A. Anderko, P. McKenzie, R. D. Young, "Computation of rates of general corrosion using electrochemical and thermodynamic models," Corrosion 57, 3 (2001) p. 202-213.

4. A. Anderko, S. J. Sanders, R. D. Young, "Real-solution stability diagrams: a thermodynamic tool for modeling corrosion in wide temperature and concentration ranges," Corrosion 53, 1 (1997) p. 43-53.

5. D. A. Wiesenburg, B. J. Little, "A synopsis of the chemical/physical properties of seawater," Ocean Physics and Engineering 12, 3&4 (1988) p. 127-165.

6. A. Anderko, P. J. Shuler, "Modeling the formation of iron sulfide scales using thermodynamic simulation software," CORROSION / 98, 64 (Houston, TX: NACE International, 1998).

7. M. B. McNeil, J. M. Jones, B. J. Little, "Mineralogical fingerprints for corrosion process induced by sulfate-reducing bacteria," CORROSION / 91, Paper no. 580 (Houston, TX: NACE International, 1991).

8. C. S. Brossia, L. Yang, "Studies of microbiologically influenced corrosion using a coupled multielectrode array sensor," CORROSION / 2003, Paper no. 03575 (Houston, TX: NACE International, 2006).

9. L. Yang, G. Cragnolino, "Studies on the corrosion behavior of stainless steels in chlroide solutions in the presence of sulfate reducing bacteria," CORROSION / 2004, paper no. 04598 (Houston, TX: NACE International, 2004).

10. B. J. Webster, R. G. Kelly, R. C. Newman, "The electrochemistry of SRB corrosion in austentic stainless steel," in Microbially Influenced Corrosion and Biodeterioration, eds. N. J. E. Dowling, M. W. Mittelman and J. C. Danko (Knoxville, TN: The University of Tennessee, 1990), p. 2/9-2/17.

11. A. Neville, T. Hodgkeiss, "Corrosion of stainless steels in marine conditions containing sulphate reducing bacteria," British Corrosion Journal 35, 1 (2000) p. 60-69.

12. S. C. Dexter, "Laboratory solutions for studying corrosion of aluminum alloys in seawater," in The Use of Synthetic Environments for Corrosion Testing, Vol. STP 970, eds. P. E. Francis and T. S. Lee (Philadelphia, PA: ASTM, 1988), p. 217-234.

13. B. J. Webster, R. C. Newman, "Producing rapid sulfate-reducing bacteria (SRB)-influenced corrosion in the laboratory," in Microbiologically Influenced Corrosion Testing, Vol. STP 1232, eds. J. R. Kearns and B. J. Little (Philadelphia, PA: ASTM, 1994), p. 28-41.

14. R. C. Salvarezza, M. F. L. de Mele, H. A. Videla, "Mechanisms of the microbial corrosion of aluminum alloys," Corrosion 39, 1 (1983) p. 26-32.

15. B. J. Little, "A perspective on the use of anion ratios to prdict corrosion in Yucca Mountain," Corrosion 59, 8 (2003) p. 701-704.

16. J. S. Lee, R. I. Ray, B. J. Little, "Comparison of Key West and Persian Gulf Seawater," CORROSION / 2007, Paper no. 07518 (Houston, TX: NACE International, 2007).

TABLES

Table 1. The Major Ions in Seawater[5]

Cations	ppm	Anions	ppm
Na^+	10779	Cl^-	19375
Mg^{2+}	1282	SO_4^{2-}	2710
Ca^{2+}	410	HCO_3^-	113
K^+	398	CO_3^{2-}	11

FIGURES

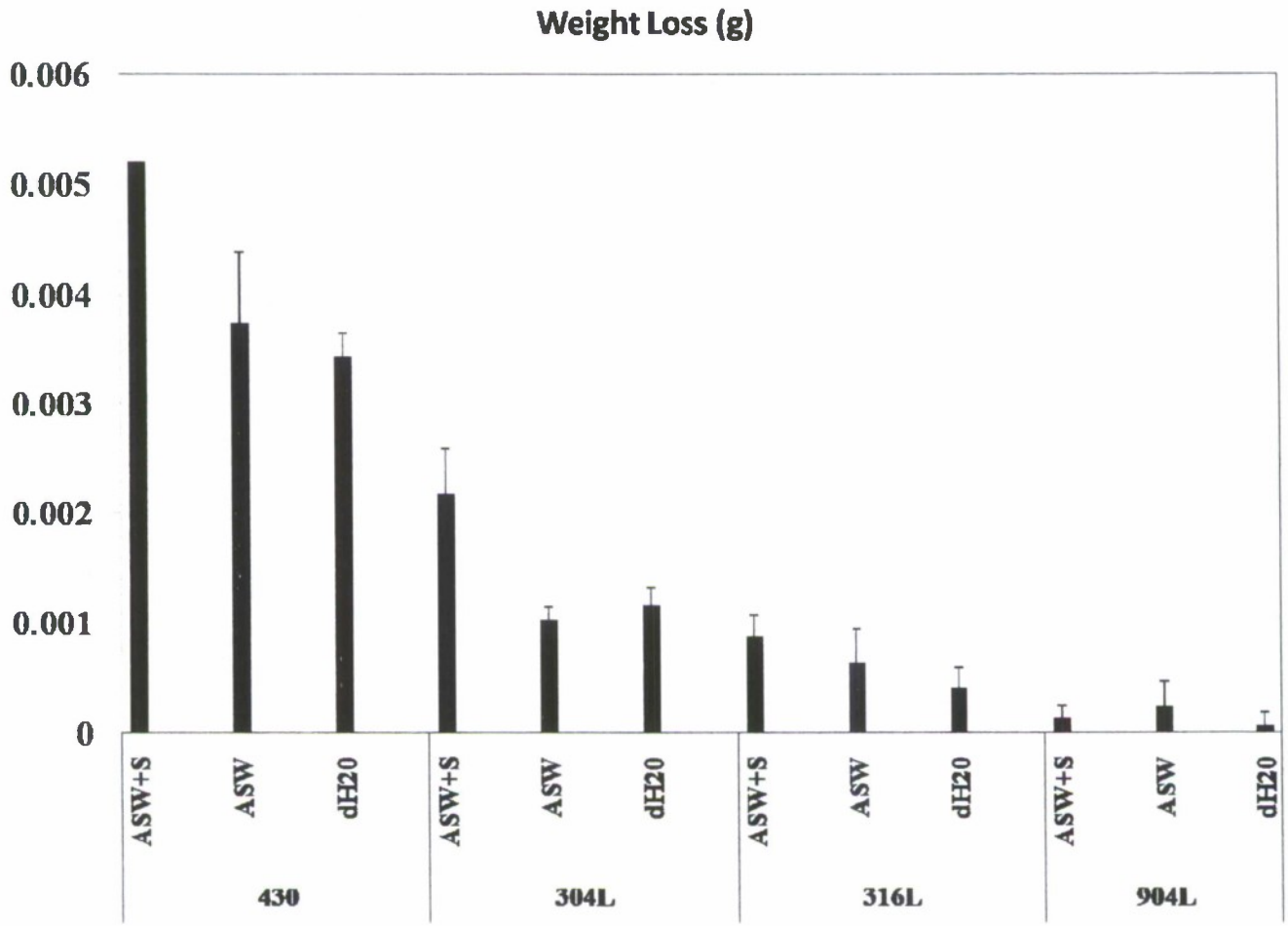

Figure 1. Average weight loss data for alloys 430, 304L, 316L, and 904L after 65 hour exposure to artificial seawater (ASW), ASW with 10^{-2}M sulfide (ASW+S), and distilled water (dH2O). Error bars represent standard deviation of triplicate samples.

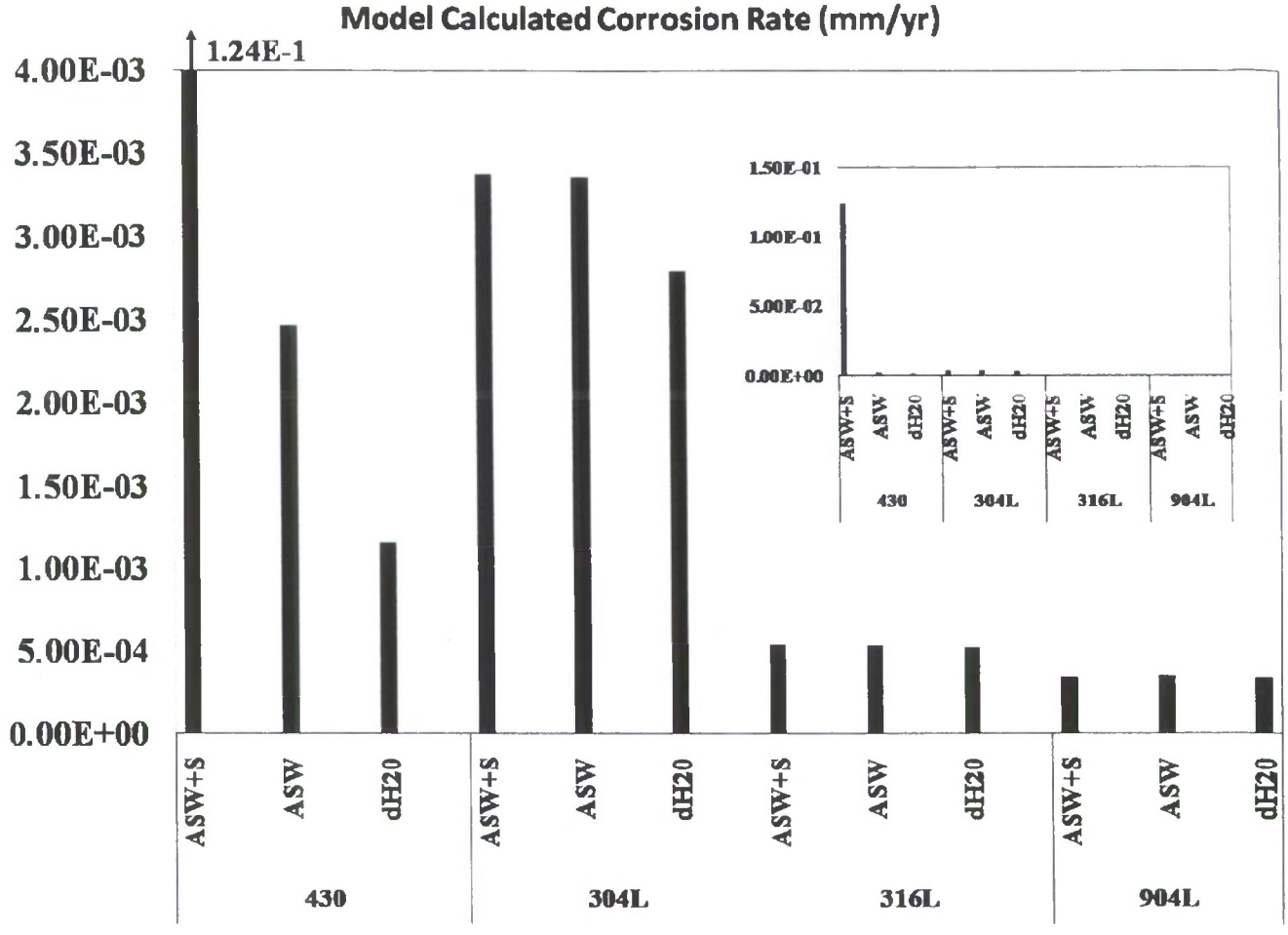

Figure 2. Calculated corrosion rates for alloys 430, 304L, 316L, and 904L after modeled exposure to artificial seawater (ASW), ASW with 10^{-2}M sulfide (ASW+S), and distilled water (dH2O). Alloy 430 was modeled using a Fe-13Cr stainless steel, while 904L was modeled using S31254 stainless steel. Inset has y-axis at full scale to show the much higher corrosion rate of 430 exposed to ASW+S.

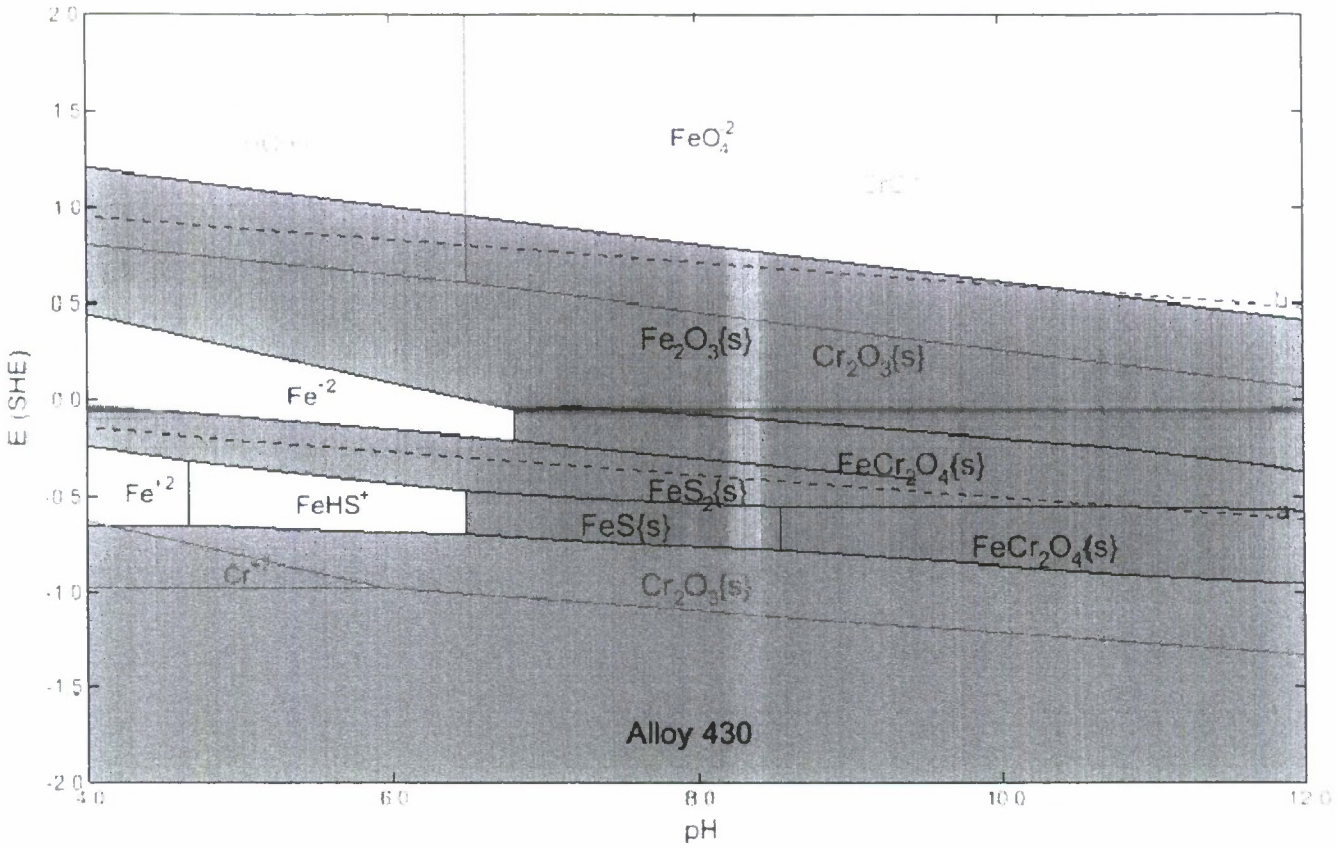

Figure 3. Stability diagram for Fe-Cr stainless steel 430 with 10^{-2}M sulfide addition. Iron subsystem solids are shown in green shading, gray shading indicates metal, and the chromium system is highlighted in light blue.

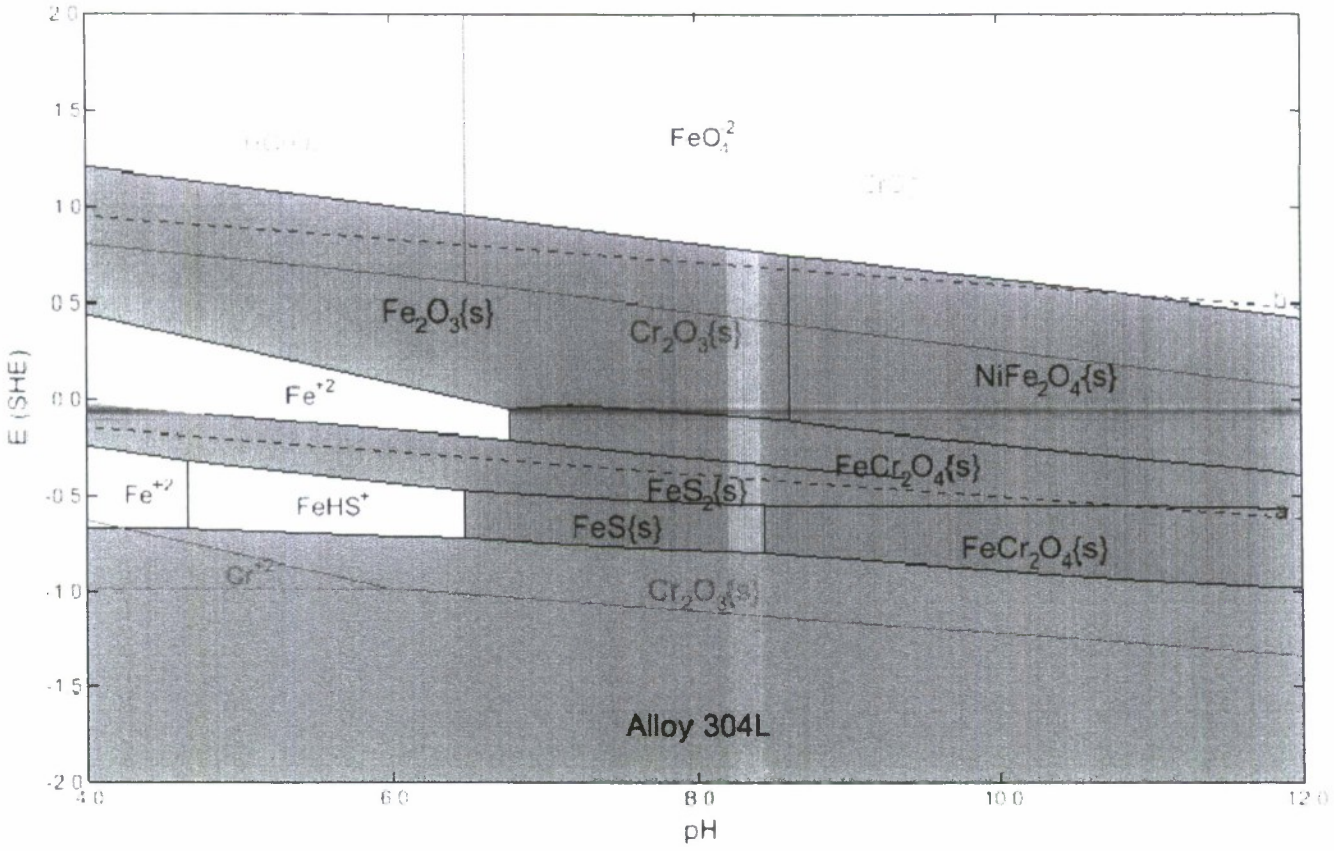

Figure 4. Stability diagram for Fe-Cr-Ni stainless steel 304L with 10^{-2}M sulfide addition. Iron subsystem solids are shown in green shading, gray shading indicates metal, and the chromium system is highlighted in light blue.

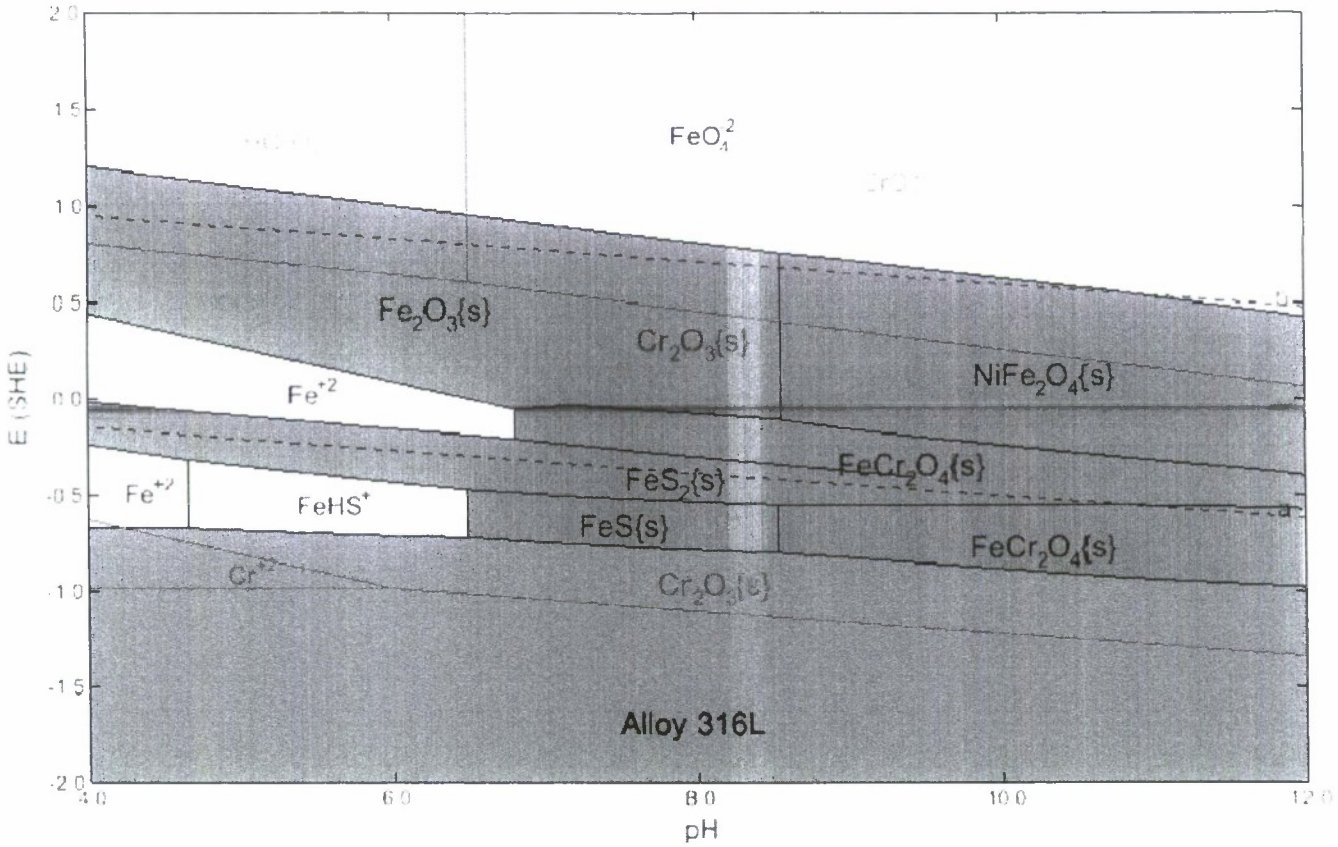

Figure 5. Stability diagram for Fe-Cr-Ni-Mo stainless steel 316L with 10^{-2}M sulfide addition. Iron subsystem solids are shown in green shading, gray shading indicates metal, and the chromium system is highlighted in light blue.

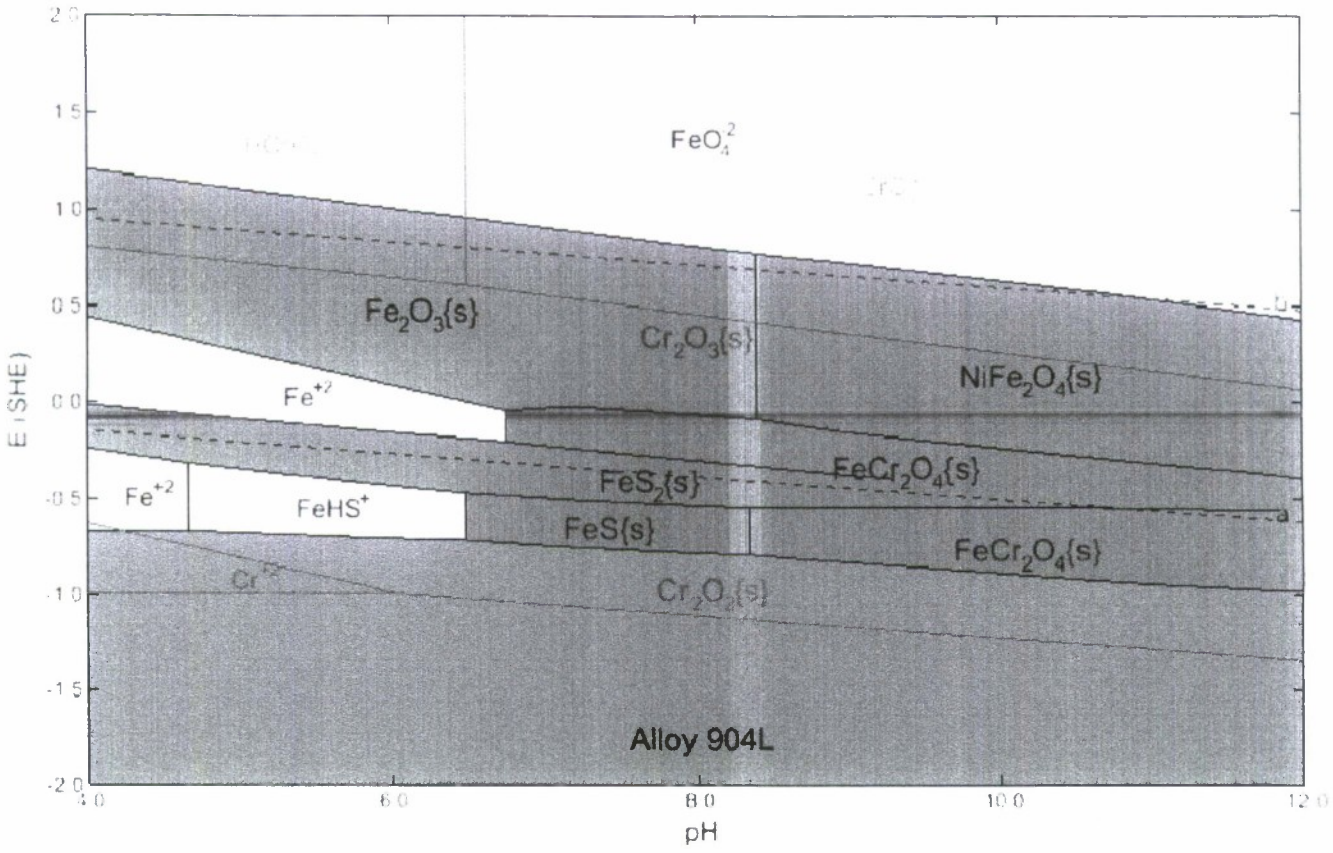

Figure 6. Stability diagram for Fe-Cr-Ni-Mo stainless steel 904L with 10^{-2}M sulfide addition. Iron subsystem solids are shown in green shading, gray shading indicates metal, and the chromium system is highlighted in light blue.